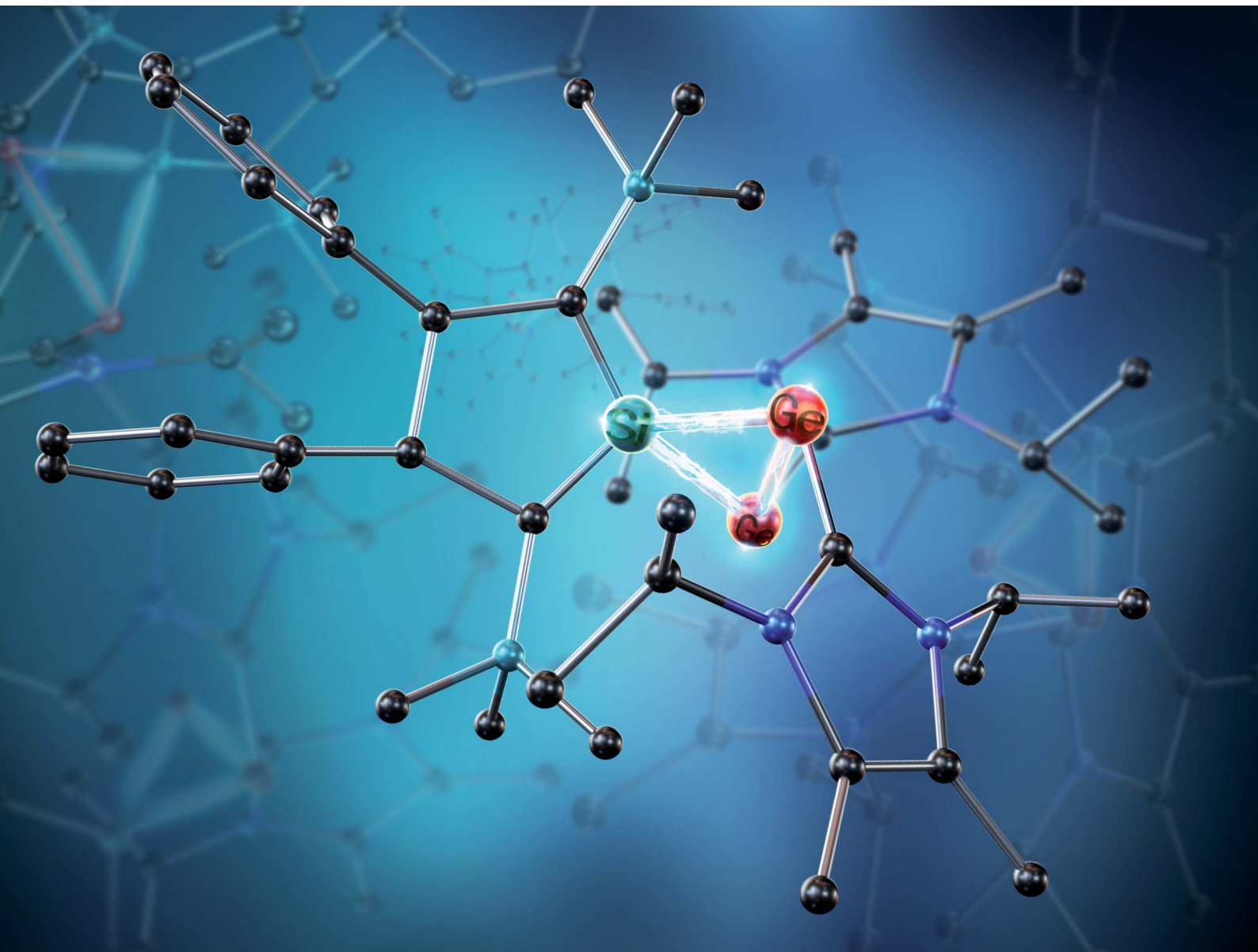


# Chemical Science

[rsc.li/chemical-science](https://rsc.li/chemical-science)



ISSN 2041-6539

Cite this: *Chem. Sci.*, 2021, **12**, 6287

All publication charges for this article have been paid for by the Royal Society of Chemistry

Received 17th February 2021  
Accepted 19th March 2021

DOI: 10.1039/d1sc00956g  
[rsc.li/chemical-science](http://rsc.li/chemical-science)

## Three-membered cyclic digermynes stabilised by an N-heterocyclic carbene<sup>†</sup>

Zhaowen Dong,<sup>ID ab</sup> Jan Mathis Winkler,<sup>a</sup> Marc Schmidtmann<sup>a</sup> and Thomas Müller<sup>ID \*a</sup>

Treatment of potassium salts of silole dianions with donor stabilised germanium dichlorides gave the anticipated silagermafulvenylidene  $R_2Si = Ge(Do)$  ( $R_2Si = 1$ -silacyclopentadienyl,  $Do = N$ -heterocyclic carbene (NHC)) only as transient intermediates in a side reaction. They were detected by NMR spectroscopy and, in one case, the formal dimer, 2,4-disila-1 $\lambda^3$ ,3 $\lambda^3$ -digermetane, was isolated. The main products of these reactions are sila-bis- $\lambda^3$ -germiranes, *i.e.* directly interconnected digermynes that are part of a three-membered ring. The structural data, supported by the results of density functional calculations confirm the digermyne nature of these products with a long inner cyclic Ge–Ge bond that decreases the inherent high ring strain in silagermiranes.

## Introduction

The unusual reactivity of compounds with low-coordinated main group elements has triggered intensive research and a great number of investigations over the last 20 years.<sup>1,2</sup> The addition of dihydrogen under ambient conditions to a digermyne<sup>3</sup> provided the blueprint for many follow-up reactivity studies on main group compounds including carbene analogues,<sup>4–10</sup> heteroalkenes and heteroalkynes,<sup>11–14</sup> and frustrated Lewis pairs.<sup>15–18</sup> Heavy vinylidenes **III**, as the formal fusion of carbene analogues **I** and heteroalkenes **II**, are, in view of their expected high reactivity, particularly interesting synthetic targets (Fig. 1). Several groups have recently reported the successful synthesis of selected examples of heavy vinylidenes **III** (Fig. 1) that include donor-stabilised (**V–VII**)<sup>19–22</sup> and not-complexed species (**IV**).<sup>23</sup>

Reduction of germanium(II) halides provides a synthetic route to dicoordinated digermanium compounds that are isomers of digermenylidenes **VIII**.<sup>24–27</sup> These germanium dimers with Ge in the formal oxidation state (+I) exist in two valence isomeric forms, digermynes **IX** and digermynes **X** (Fig. 2).<sup>28,29</sup> The digermylene isomer **X** is preferred when the substituent R is a multidentate ligand.<sup>30–39</sup>

Following previous investigations from our laboratory,<sup>40</sup> we probed the potential of salt metathesis of group 14 element

dianions **XI** with group 14 element dihalides **XII** followed by 1,2-elimination for the synthesis of heavy vinylidenes **III** (Fig. 3). In contrast to our expectations, two single salt metathesis reactions occurred and the isolated products after subsequent reduction by the excess dianion were cyclic ditetrylenes **XIII**.

## Results and discussion

The starting materials of choice for us were silole dianions<sup>41</sup> and germanium dichloride stabilised by N-heterocyclic carbenes (NHC).<sup>42,43</sup> The reaction of dipotassium silacyclopentadienides  $K_2[1]$  with NHC-stabilised dichlorogermylene **2** gave the 3-sila-1 $\lambda^3$ ,2 $\lambda^3$ -digermiranes **5** as main products (Scheme 1). Deep green crystals of siladigermiranes **5** were obtained by recrystallization from diethyl ether at  $-30\text{ }^\circ\text{C}$  in 23% (**5a**) and 64% (**5b**) yields. Both spiro-heterocycles were characterised by NMR and UV spectroscopy, MS spectrometry and X-ray diffraction analysis (XRD) of suitable single crystals.<sup>29</sup> Si NMR data of siladigermiranes **5** are unremarkable and compare well with

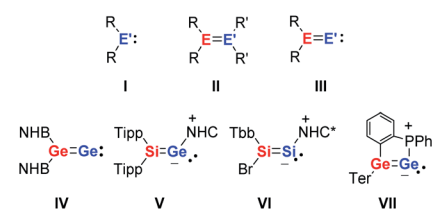


Fig. 1 Carbene analogues **I**, heteroalkenes **II**, heavy vinylidenes **III** ( $E, E' = Si, Ge$ ) and some examples of isolable sila- and germavinylenes (**IV–VII**) ( $NHB = (HC(Dipp)N)_2B$ ,  $Tipp = 2,4,6$ -trisopropylphenyl,  $NHC = (MeC(iPr)N)_2C$ ,  $Tbb = 2,6$ -(( $Me_3Si)_2CH)_2-4-tert-butylphenyl,  $NHC^* = (H_2C(Dipp)N)_2C$ ,  $Ter = 2,6$ -bis(2,4,6-trisopropylphenyl)phenyl, and  $Dipp = 2,6$ -diisopropylphenyl).$

<sup>a</sup>Institute of Chemistry, Carl von Ossietzky University of Oldenburg, Carl von Ossietzky-Str. 9-11, D-26129 Oldenburg, Federal Republic of Germany. E-mail: thomas.mueller@uni-oldenburg.de

<sup>b</sup>Institut des Sciences et Ingénierie Chimiques, Ecole Polytechnique Fédérale de Lausanne (EPFL), 1015 Lausanne, Switzerland

† Electronic supplementary information (ESI) available. CCDC 1893832–1893834. For ESI and crystallographic data in CIF or other electronic format see DOI: 10.1039/d1sc00956g



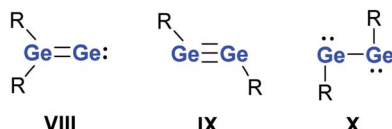


Fig. 2 Digermenylidenes VIII, digermynes IX and digermynes X.

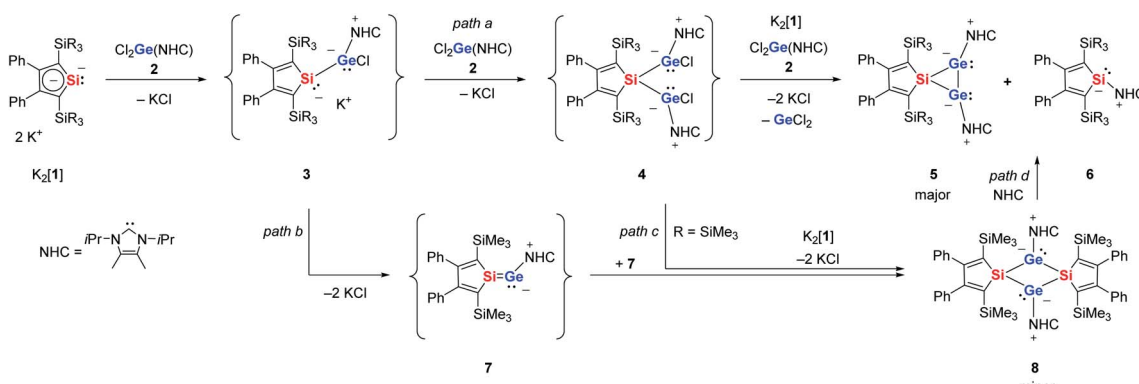
Fig. 3 Attempted synthesis of heavy vinylidenes by double salt metathesis and formation of cyclic ditetylenes after salt metathesis and reduction ( $E, E' = Si, Ge$ ).

those of previously reported siladigermiranes.<sup>44–46</sup> The  $^{13}C$  NMR data indicate a silole group with localized  $C=C$  double bonds (see the ESI material†). The green colour of these compounds results from broad long-wave absorptions at  $\lambda_{max} = 610$  nm (**5a**) and  $\lambda_{max} = 625$  nm (**5b**). During the reaction of  $K_2[1a]$  with dichlorogermylene **2**, the known NHC-stabilised silylene **6a** was detected by NMR spectroscopy as a by-product and was identified by comparison with literature data.<sup>47</sup> After isolation of compound **5a**, crystallization from diethyl ether allowed a second crop of a few dark red crystals of the tricyclic compound **8** that was identified by XRD analysis (Scheme 1). When the reaction of  $K_2[1a]$  and dichlorogermylene **2** was followed by NMR spectroscopy, already at  $-30^\circ C$  a mixture of products was detected (see ESI† for details). The  $^{29}Si\{^1H\}$  inverse gated NMR spectra indicated the presence of the NHC-stabilised silylene **6a** ( $\delta^{29}Si = -32.9$  (SiC<sub>4</sub>),  $-11.8$ ), of the bicyclic siladigermirane **5a** ( $\delta^{29}Si = -9.8$ ,  $-7.0$  (SiC<sub>4</sub>)) and of the tricyclic disilagermetane **8** ( $\delta^{29}Si = +6.0$  (SiC<sub>4</sub>),  $-7.8$ ). Besides these signals, there are three additional resonances at  $\delta^{29}Si = +157.9$  (SiC<sub>4</sub>),  $-3.5$  and  $-6.1$  (see Fig. S1b† for details). The low field signal is in a typical region for silicon atoms involved in multiple bonds and very close to the  $^{29}Si$  NMR chemical shift reported by the Scheschkewitz group for the NHC-stabilised silagermenylidene **9** ( $\delta^{29}Si(9) = 159$ ).<sup>19</sup> At reaction

temperatures above  $-30^\circ C$  and prolonged reaction time, the intensity of these signals steadily decreased. Based on the low field  $^{29}Si$  NMR resonance, we identified this intermediate as the NHC stabilised silagermenylidene **7**. This assignment is supported by NMR chemical shift calculations, which predict for the tricoordinated silicon atom of silagermenylidene **7**  $\delta^{29}Si(\text{calc}) = 178$ , close to the experimental value (see ESI†).

Based on these experimental observations, we suggest for this complex reaction the following course (Scheme 1). The main product **5** is formed by two subsequent salt metathesis reactions *via* the germyl chlorides **3** and **4** (Scheme 1, *path a*). Such twofold salt metathesis reactions have precedence in stannole dianion chemistry.<sup>48</sup> The dichlorides **4** undergo a reductive dehalogenation to form the three-membered ring compounds **5**. At this point, the silole dianions **1** act as reducing agents and the NHC-stabilised silylenes **6** are obtained as by-products. The transient silagermenylidene **7** is formed by salt elimination from chloride **3a** and subsequently it dimerized to give disilagermetane **8** (Scheme 1, *path b*). In view of the very low yield of **8**, we suggest that this is only one of several reaction channels for silagermenylidene **7**. Likewise, we cannot exclude that compound **8** is formed by double salt metathesis of digermyl chloride **4** with the starting material  $K_2[1]$  (Scheme 1, *path c*). Based on the result of DFT calculations, we can discard the possibility of a reversible dimerization of silagermenylidene **7**, as the dimerization is highly exothermic and exergonic ( $\Delta E = -266$  kJ mol<sup>-1</sup>,  $\Delta G = -160$  kJ mol<sup>-1</sup> ( $T = 298$  K), see Fig. S7†). On the other hand, the formation of disilagermirane **5a** from disilagermetane **8** by reaction with NHC (Scheme 1, *path d*) is thermodynamically feasible as it is only slightly endothermic ( $\Delta E = 22$  kJ mol<sup>-1</sup>,  $\Delta G = 3$  kJ mol<sup>-1</sup> ( $T = 298$  K), see Fig. S7†). We were not able to improve the yields of products **5** by adjusting the stoichiometry of the reaction according to the reaction course shown in Scheme 1. This suggests similar activation barriers for the competing reaction channels. Increasing the steric bulk of the N-heterocyclic carbene resulted in no reaction between the NHC-stabilised germanium dichloride and the dianion even at the temperature of boiling THF.

Deep green single crystals suitable for X-ray diffraction (XRD) analysis were obtained for both siladigermiranes **5** from

Scheme 1 Reaction of dipotassium silole dianions  $K_2[1]$  with NHC-stabilised dichlorogermylene **2** (a:  $R = Me$ ; b:  $R = Et$ ).

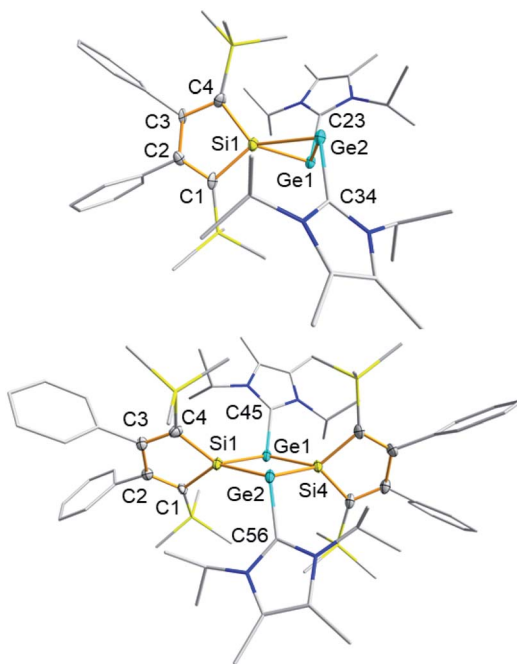


Fig. 4 Top: molecular structures of 3-sila-1 $\lambda^3$ ,2 $\lambda^3$ -digermirane 5a in the crystal (thermal ellipsoids at 50% probability, all hydrogen atoms are omitted for clarity. The NHC, Me<sub>3</sub>Si and Ph substituents are simplified as a wireframe). Selected atomic distances [pm] and angles [ $^\circ$ ]: Ge1–Ge2 259.3(11), Si1–Ge1 244.6(2), Si1–Ge2 242.5(2), Ge1–C23 203.7(7), Ge2–C34 203.5(7), C23–Ge1–Ge2 96.59(20), C34–Ge2–Ge1 100.98(20), and  $\alpha$ (SiC<sub>4</sub>/SiGe<sub>2</sub>) 68.3. Bottom: molecular structure of 2,3-disila-1 $\lambda^3$ ,3 $\lambda^3$ -digermetane 8 in the crystal (thermal ellipsoids at 50% probability, all hydrogen atoms are omitted for clarity. NHC substituents are simplified as a wireframe). Selected atomic distances [pm] and angles [ $^\circ$ ]: Si1–Ge1 246.2(12), Si1–Ge2 245.0(16), Si4–Ge1 244.3(16), Si4–Ge2 243.1(16), Ge1–Ge2 339.8(11), Si1–Si4 352.1(20), Ge1–C45 200.2(6), Ge2–C56 201.6(5), C45–Ge1–Ge2 122.54(14), C56–Ge2–Ge1 122.74(14), and  $\alpha$ (SiC<sub>4</sub>/Si<sub>2</sub>Ge<sub>2</sub>) 58.3.

concentrated Et<sub>2</sub>O solutions. Their molecular structures in the crystal are very similar and we discuss here only that of siladigermirane 5a in detail (Fig. 4, for details on the crystal structure of siladigermirane 5b, see ESI†). The molecule is almost  $C_2$ -symmetric and its most prominent feature is the three membered SiGe<sub>2</sub>-ring with a very long Ge–Ge bond of 259.3 pm, which is longer by 7% than a regular Ge–Ge single bond (242 pm).<sup>49</sup> It is however shorter by 28.4 pm than what is found for the Ge–Ge separation in dianion 10 (Ge–Ge = 287.7 pm, Fig. 5)<sup>50</sup> and also significantly shorter than the Ge–Ge distance in the

neutral germanium(i) dimer 11 (Ge–Ge = 270.9 pm).<sup>26</sup> In addition, the Si–Ge bonds in siladigermirane 5a are slightly elongated compared to standard values (mean value in 5a 243.6 pm vs. standard value 237 pm).<sup>49</sup> In summary, the metrics of the SiGe<sub>2</sub> ring are close to those reported for 3,3-di-*tert*-butyl-tetramesityl-3-siladigermirane.<sup>45</sup> The imidazolium substituents are oriented in a *trans*-arrangement and the Ge–C bonds (mean value 203.6 pm) are typically longer than the standard value (Ge–C = 196 pm).<sup>43,49</sup> The C–Ge–Ge bond angles are small (96.6° and 101.0°) and both rings of the spiro compound enclose a dihedral angle of 68.3°. The coordination environment of the germanium atoms in 5a indicates the presence of a non-bonded electron pair at each of them. This is in agreement with the notion of siladigermiranes 5 as interconnected cyclic digermynes, which are stabilised by the interaction with two NHCs.

Dark red single crystals of disiladigermetane 8 suitable for XRD analysis were obtained from the mother liquor of siladigermirane 5a at –30 °C. The dominant feature of the molecular structure of 8 is the almost quadratic (SiGe)<sub>2</sub> four-membered ring (Fig. 3). The two silole rings are tilted by 58.3° against this central ring. The Si–Ge bonds are slightly longer (by 3–4%) than the standard value. The *trans*-cyclic Ge–Ge (339.8 pm) and Si–Si distances (352.1 pm) are smaller than the sum of the van der Waals radii ( $\Sigma$ v<sub>dw</sub>(SiSi): 420 pm,  $\Sigma$ v<sub>dw</sub>(GeGe): 422 pm)<sup>51</sup> but are longer by 40% (GeGe) and 52% (SiSi) than their respective single bonds.<sup>49</sup> This excludes *trans*-cyclic bonding interaction between these atoms. Similar to the siladigermiranes 5, the NHC-substituents are arranged in a *trans* fashion at the two Ge-atoms with typically long Ge–C(NHC) bonds. The C–Ge–Ge angles are however less acute (122.5 and 122.7°) and the coordination environment around the two germanium atoms is trigonal pyramidal (sum of the bond angles around germanium,  $\Sigma\alpha$ (Ge) = 316.0 and 316.4°).

Quantum mechanical calculations at the density functional M06-2X/Def2-TZVP for 5a and for the model siladigermirane 12 were used to investigate the electronic nature of the spiro compounds 5 (see ESI†). The molecular structures optimized for 5a and 12 at this level of theory agree well with the experimental structures that are obtained from XRD analysis. The largest deviation in bond lengths is found for the Ge–C(NHC) linkage showing germanium carbon distances that are elongated by 2% (5a) and by 1% (12) compared to the experimental structure of 5a (see Table S4†). The mean bond dissociation energy (BDE) of the Ge–C(NHC) bond calculated for model compound 12 is substantial (BDE(mean) = 251 kJ mol<sup>–1</sup>). This indicates the strong stabilization of the siladigermirane by the two NHC substituents at the low coordinated germanium centres. The HOMO of compound 12 is almost exclusively the Ge–Ge  $\sigma$ -bond which is a combination of the atomic Ge(4p) orbitals that are oriented perpendicular to the respective Ge–Si vector. Consequently, the HOMO is slightly bent away from the centre of the three membered ring (Fig. 6). The atomic Ge(4s) orbitals dominate the HOMO–2. The shapes of the HOMO–1 and the LUMO indicate the cross-hyperconjugation between the silole ring and the Ge–Si  $\sigma$ -bonds of the three membered ring (Fig. 6).<sup>52,53</sup> A population analysis in the framework of natural bond orbital (NBO) theory<sup>54</sup> suggests that the Ge–Ge  $\sigma$ -bond is

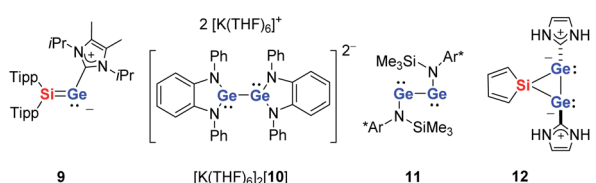


Fig. 5 Compounds that are of relevance for the discussion (Tipp: 2,4,6-triisopropylphenyl, Ar\*: 2,6-bisdiphenylmethyl-4-methylphenyl).

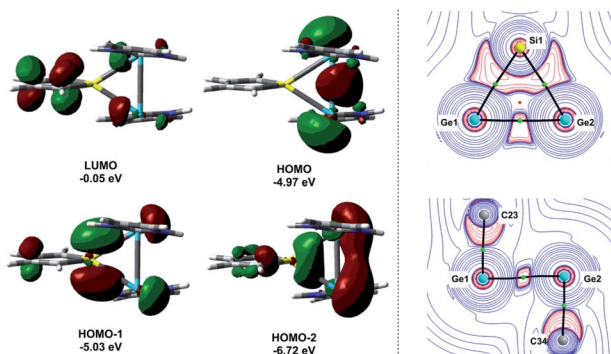


Fig. 6 Left: calculated surface diagrams of the frontier molecular orbitals of siladigermirane 12 (isodensity value 0.04, at M06-2X/Def2-TZVP). Right: 2D contour plots of the calculated Laplacian of the electron density,  $\nabla^2 \rho(r)$ , in the Ge1–Si1–Ge2 plane (top) and in the Ge1–Ge2–C34 plane (bottom) of model compound 12. The molecular graph of model 12 is projected onto the respective contour plot. Solid black lines show the bond paths, which follow the line of maximum electron density between bonded atoms. The corresponding bond critical points (BCP's) are shown as green circles, and ring critical points as red spheres. Red contours indicate regions of local charge accumulation ( $\nabla^2 \rho(r) < 0$ ); blue contours indicate regions of local charge depletion ( $\nabla^2 \rho(r) > 0$ ).

composed of almost exclusively Ge(4p) orbitals (94% p-orbital contribution, Fig. S9†). The lone pairs at both germanium atoms show large contributions of the 4s(Ge) atomic orbitals (79% s-, 21% p-orbital contribution). The calculated Wiberg bond index (WBI) of the Ge–Ge bond in 12 is very close to that of typical Ge–Ge single bonds (WBI = 0.84 (12) vs. 0.89 (13) and 0.92 (14), Table 1).<sup>55</sup> From the wavefunction-based analysis, it is apparent that the long Ge–Ge bond in model compound 12 and likewise in siladigermiranes 5 is the result of the almost pure p-orbital contributions. The complementary analysis of the calculated electron density (quantum theory of atoms in molecules, QTAIM) identifies the Ge–Ge bond in 12 by its properties at the bond critical point (BCP) as being non-polar and covalent

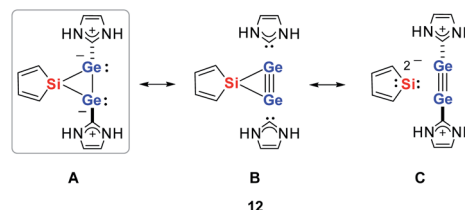


Fig. 7 Possible resonance structures of 3-sila-1λ³,2λ³-digermirane 12.

(significant electron density  $\rho$ , negative Laplacian  $\nabla^2 \rho$ , negative total energy density  $H$ , see Table 1 and ESI†).<sup>56</sup> The electron density at the BCP is however small compared to that calculated for the typical Ge–Ge bond in hexamethyl digermane, 13, and for the Ge–Ge bond in siladigermirane 14. Noticeable is the non-spherical electron distribution at the BCP as expressed by the large ellipticity  $\varepsilon$  of the electron density at the BCP. It is larger than calculated for the  $\pi$ -bond in siladigermirene 15 and the accumulation of charge extends into an area in the plane of the three-membered ring and directed away from its centre in agreement with the shape of the  $\sigma$ -Ge–Ge bond (Fig. 5). Consistent with the analysis of the experimental structure, the computational results indicate the digermylene nature of compounds 5 and 12 with the two germylene centres interconnected by a Ge–Ge  $\sigma$ -bond as represented by the canonical structure 12A (Fig. 7). Contributions of resonance structures with multiple bonds between the germanium atoms (i.e. 12B and 12C) are negligible.

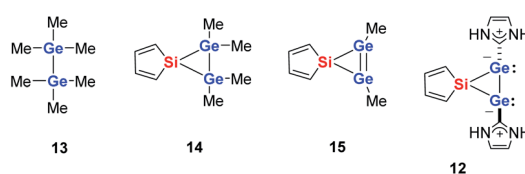
As the ring strain in heavy cyclopropanes ( $E_3H_6$ ,  $E = Si, Ge$ ) is considerably higher than that of cyclopropane (162–165 kJ mol<sup>-1</sup> vs. 124 kJ mol<sup>-1</sup> for  $C_3H_6$ ),<sup>57,58</sup> we studied the influence of the integration of the  $Ge_2$  unit in a three-membered ring using a set of isodesmic reactions. We found that the long Ge–Ge bond reduces the ring strain in siladigermirane 12 by 32 kJ mol<sup>-1</sup> compared to a related siladigermirane (see ESI† for details). This factor contributes to the thermodynamic stability of this unusual  $SiGe_2$  cycle.

## Conclusions

The reaction of  $K_2[1]$  with NHC stabilised germanium dichloride yields 3-sila-1λ³,2λ³-digermiranes 5 as main products. The targeted silagermylidene 7 was detected only as an intermediate in a side reaction by NMR spectroscopy. Based on the analysis of the structural and computational data the three-membered ring compounds 5 are directly interconnected digermylenes that are stabilised by NHCs.

## Author contributions

Z. D. was responsible for experimental investigations and formal analysis (lead), computational investigation and visualization, data presentation and writing original draft (equal with T. M.), methodology and conceptualization (supportive). J. M. W. was responsible for experimental investigations (supportive) and validation. M. S. collected the X-ray data and solved the



crystal structures. T. M. was in charge for methodology and conceptualization, computational investigations, review and editing of the manuscript (lead), project administration and funding acquisition.

## Conflicts of interest

There are no conflicts to declare.

## Acknowledgements

Z. D. thanks the state of Lower Saxony for a Georg Lichtenberg Scholarship. This work was supported by the Deutsche Forschungsgemeinschaft (DFG-Mu1440/13-1 and INST 184/108-1 FUGG).

## References

- 1 P. P. Power, *Nature*, 2010, **463**, 171–177.
- 2 T. Chu and G. I. Nikonov, *Chem. Rev.*, 2018, **118**, 3608–3680.
- 3 G. H. Spikes, J. C. Fettinger and P. P. Power, *J. Am. Chem. Soc.*, 2005, **127**, 12232–12233.
- 4 G. D. Frey, V. Lavallo, B. Donnadieu, W. W. Schoeller and G. Bertrand, *Science*, 2007, **316**, 439–441.
- 5 D. Martin, M. Soleilhavoup and G. Bertrand, *Chem. Sci.*, 2011, **2**, 389–399.
- 6 M. Melaimi, R. Jazzar, M. Soleilhavoup and G. Bertrand, *Angew. Chem., Int. Ed.*, 2017, **56**, 10046–10068.
- 7 Y. Mizuhata, T. Sasamori and N. Tokitoh, *Chem. Rev.*, 2009, **109**, 3479–3511.
- 8 M. Asay, C. Jones and M. Driess, *Chem. Rev.*, 2011, **111**, 354–396.
- 9 T. J. Hadlington, J. A. B. Abdalla, R. Tirfoin, S. Aldridge and C. Jones, *Chem. Commun.*, 2016, **52**, 1717–1720.
- 10 D. Wendel, A. Porzelt, F. A. D. Herz, D. Sarkar, C. Jandl, S. Inoue and B. Rieger, *J. Am. Chem. Soc.*, 2017, **139**, 8134–8137.
- 11 P. P. Power, *Acc. Chem. Res.*, 2011, **44**, 627–637.
- 12 D. Wendel, T. Szilvási, C. Jandl, S. Inoue and B. Rieger, *J. Am. Chem. Soc.*, 2017, **139**, 9156–9159.
- 13 B. Wang, Y. Li, R. Ganguly, H. Hirao and R. Kinjo, *Nat. Commun.*, 2016, **7**, 11871.
- 14 T. Kosai and T. Iwamoto, *J. Am. Chem. Soc.*, 2017, **139**, 18146–18149.
- 15 D. W. Stephan and G. Erker, *Angew. Chem., Int. Ed.*, 2015, **54**, 6400–6441.
- 16 D. W. Stephan, *J. Am. Chem. Soc.*, 2015, **137**, 10018–10032.
- 17 D. W. Stephan, *Acc. Chem. Res.*, 2015, **48**, 306–316.
- 18 D. W. Stephan, *Science*, 2016, **354**, aaf7229.
- 19 A. Jana, V. Huch and D. Scheschke, *Angew. Chem., Int. Ed.*, 2013, **52**, 12179–12182.
- 20 A. Jana, M. Majumdar, V. Huch, M. Zimmer and D. Scheschke, *Dalton Trans.*, 2014, **43**, 5175–5181.
- 21 P. Ghana, M. I. Arz, U. Das, G. Schnakenburg and A. C. Filippou, *Angew. Chem., Int. Ed.*, 2015, **54**, 9980–9985.
- 22 K. M. Krebs, D. Hanselmann, H. Schubert, K. Wurst, M. Scheele and L. Wesemann, *J. Am. Chem. Soc.*, 2019, **141**, 3424–3429.
- 23 A. Rit, J. Campos, H. Niu and S. Aldridge, *Nat. Chem.*, 2016, **8**, 1022–1026.
- 24 M. Stender, A. D. Phillips, R. J. Wright and P. P. Power, *Angew. Chem., Int. Ed.*, 2002, **41**, 1785–1787.
- 25 Y. Sugiyama, T. Sasamori, Y. Hosoi, Y. Furukawa, N. Takagi, S. Nagase and N. Tokitoh, *J. Am. Chem. Soc.*, 2006, **128**, 1023–1031.
- 26 J. Li, C. Schenk, C. Goedecke, G. Frenking and C. Jones, *J. Am. Chem. Soc.*, 2011, **133**, 18622–18625.
- 27 T. J. Hadlington, M. Hermann, J. Li, G. Frenking and C. Jones, *Angew. Chem., Int. Ed.*, 2013, **52**, 10199–10203.
- 28 R. C. Fischer and P. P. Power, *Chem. Rev.*, 2010, **110**, 3877–3923.
- 29 Y. Peng, R. C. Fischer, W. A. Merrill, J. Fischer, L. Pu, B. D. Ellis, J. C. Fettinger, R. H. Herber and P. P. Power, *Chem. Sci.*, 2010, **1**, 461–468.
- 30 S. Nagendran, S. S. Sen, H. W. Roesky, D. Koley, H. Grubmüller, A. Pal and R. Herbst-Irmer, *Organometallics*, 2008, **27**, 5459–5463.
- 31 W. Wang, S. Inoue, S. Yao and M. Driess, *Chem. Commun.*, 2009, 2661–2663.
- 32 W.-P. Leung, W.-K. Chiu, K.-H. Chong and T. C. W. Mak, *Chem. Commun.*, 2009, 6822–6824.
- 33 C. Jones, S. J. Bonyhady, N. Holzmann, G. Frenking and A. Stasch, *Inorg. Chem.*, 2011, **50**, 12315–12325.
- 34 S.-P. Chia, H.-X. Yeong and C.-W. So, *Inorg. Chem.*, 2012, **51**, 1002–1010.
- 35 M. Novák, M. Bouška, L. Dostál, A. Růžička, A. Hoffmann, S. Herres-Pawlis and R. Jambor, *Chem.-Eur. J.*, 2015, **21**, 7820–7829.
- 36 W.-P. Leung, W.-K. Chiu and T. C. W. Mak, *Organometallics*, 2014, **33**, 225–230.
- 37 X. Wang, J. Liu, J. Yu, L. Hou, W. Sun, Y. Wang, S. Chen, A. Li and W. Wang, *Inorg. Chem.*, 2018, **57**, 2969–2972.
- 38 S. Kundu, P. P. Samuel, A. Luebben, D. M. Andrade, G. Frenking, B. Dittrich and H. W. Roesky, *Dalton Trans.*, 2017, **46**, 7947–7952.
- 39 S. P. Green, C. Jones, P. C. Junk, K.-A. Lippert and A. Stasch, *Chem. Commun.*, 2006, 3978–3980.
- 40 Z. Dong, L. Albers and T. Müller, *Acc. Chem. Res.*, 2020, **53**, 532–543.
- 41 Z. Dong, C. R. W. Reinhold, M. Schmidtmann and T. Müller, *Organometallics*, 2018, **37**, 4736–4743.
- 42 P. A. Rupar, V. N. Staroverov, P. J. Ragogna and K. M. Baines, *J. Am. Chem. Soc.*, 2007, **129**, 15138–15139.
- 43 V. Nesterov, D. Reiter, P. Bag, P. Frisch, R. Holzner, A. Porzelt and S. Inoue, *Chem. Rev.*, 2018, **118**, 9678–9842.
- 44 K. M. Baines and J. A. Cooke, *Organometallics*, 1991, **10**, 3419–3421.
- 45 G. M. Kolleger, W. G. Stibbs, J. J. Vittal and K. M. Baines, *Main Group Met. Chem.*, 1996, **19**, 317–330.
- 46 S. E. Gottschling, A. J. Guiernau Jacobs, M. C. Jennings and K. M. Baines, *Silicon Chem.*, 2002, **1**, 1–21.



47 D. Tian, X. Li, Y. Liu, Y. Cao, T. Li, H. Hu and C. Cui, *Dalton Trans.*, 2016, **45**, 18447–18449.

48 T. Kuwabara and M. Saito, *Organometallics*, 2015, **34**, 4202–4204.

49 P. Pyykkö and M. Atsumi, *Chem.–Eur. J.*, 2009, **15**, 12770–12779.

50 M. Ma, L. Shen, H. Wang, Y. Zhao, B. Wu and X.-J. Yang, *Organometallics*, 2020, **39**, 1440–1447.

51 M. Mantina, A. C. Chamberlin, R. Valero, C. J. Cramer and D. G. Truhlar, *J. Phys. Chem. A*, 2009, **113**, 5806–5812.

52 R. Emanuelsson, A. Wallner, E. A. M. Ng, J. R. Smith, D. Nauroozi, S. Ott and H. Ottosson, *Angew. Chem., Int. Ed.*, 2013, **52**, 983–987.

53 A. V. Denisova, J. Tibbelin, R. Emanuelsson and H. Ottosson, *Molecules*, 2017, **22**, 370.

54 A. E. Reed, L. A. Curtiss and F. Weinhold, *Chem. Rev.*, 1988, **88**, 899–926.

55 K. B. Wiberg, *Tetrahedron*, 1968, **24**, 1083–1096.

56 P. Macchi and A. Sironi, *Coord. Chem. Rev.*, 2003, **238–239**, 383–412.

57 S. Nagase, *Acc. Chem. Res.*, 1995, **28**, 469–476.

58 D. A. Horner, R. S. Grev and H. F. Schaefer, *J. Am. Chem. Soc.*, 1992, **114**, 2093–2098.

